Heliyon 10 (2024) e37014

Contents lists available at ScienceDirect

Heliyon

journal homepage: www.cell.com/heliyon

Research article

Development of biomaterial composite hydrogel as a passive sampler with potential application in wastewater-based surveillance

Orlando de la Rosa [a,b], Alberto Aguayo-Acosta [a,b], Hiram Martín Valenzuela-Amaro [a,b], Edgar Ricardo Meléndez-Sánchez [a,b], Juan Eduardo Sosa-Hernández [a,b,*], Roberto Parra-Saldívar [a,b,**]

[a] Tecnologico de Monterrey, Institute of Advanced Materials for Sustainable Manufacturing, Mexico
[b] Tecnologico de Monterrey, School of Engineering and Sciences, Monterrey, 64849, Mexico

ARTICLE INFO

Keywords:
Gene adsorption
Passive sampler
Composite hydrogel
Wastewater-based surveillance

ABSTRACT

Nowadays, the need to track fast-spreading infectious diseases has raised due to the recent COVID-19 disease pandemic. As a response, Wastewater-based Surveillance (WBS) has emerged as an early detection and disease tracking method for large populations that enables a comprehensive overview of public health allowing for a faster response from public health sector to prevent large outbreaks. The process to achieve WBS requires a highly intensive sampling strategy with either expensive equipment or trained personnel to continuously sample. The sampling problem can be addressed by passive sampler development. Chitosan-based hydrogels are recognized for their capability to sample and remove various contaminants from wastewater, including metals, dyes, pharmaceuticals, among others. However, chitosan-based hydrogels unique characteristics, can be exploited to develop passive samplers of genetic material that can be a very valuable tool for WBS. This study aimed to develop a novel chitosan hydrogel formulation with enhanced characteristics suitable for use as a passive sampler of genetic material and its application to detect disease-causing pathogens present in wastewater. The study evaluates the effect of the concentration of different components on the formulation of a Chitosan composite hydrogel (Chitosan, Glutaraldehyde, Microcrystalline cellulose (MCC), and Polyethylene glycol (PEG)) on the hydrogel properties using a Box Hunter & Hunter experimental matrix. Hydrogels' weight, thickness, swelling ratio, microscopic morphology (SEM), FTIR assay, and zeta potential were characterized. The resulting hydrogel formulations were shown to be highly porous, positively charged (Zeta potential up to 35.80 ± 1.44 mV at pH 3) and with high water swelling capacity (up to 703.89 ± 15.00 %). Based on the results, a formulation from experimental design was selected and then evaluated its capacity to adsorb genetic material from a control spiked water with Influenza A virus synthetic vector. The adsorption capacity of the selected formulation was 4157.04 ± 64.74 Gene Copies/mL of Influenza A virus synthetic vector. The developed hydrogel showed potential to be used as passive sampler for pathogen detection in wastewater.

* Corresponding author. Tecnologico de Monterrey, Institute of Advanced Materials for Sustainable Manufacturing, Mexico.
** Corresponding author. Tecnologico de Monterrey, Institute of Advanced Materials for Sustainable Manufacturing, Mexico.
E-mail addresses: eduardo.sosa@tec.mx (J.E. Sosa-Hernández), ibqrps@gmail.com (R. Parra-Saldívar).

https://doi.org/10.1016/j.heliyon.2024.e37014
Received 7 March 2024; Received in revised form 8 July 2024; Accepted 26 August 2024
Available online 2 September 2024

However, deeper research can be conducted to improve adsorption, desorption and extraction techniques of genetic material from chitosan-hydrogel matrices.

1. Introduction

Wastewater-based Surveillance (WBS), formerly known as Wastewater-based epidemiology (WBE) has been a very effective monitoring strategy for disease spreading and outbreak prevention, recently more importantly in the context of the coronavirus disease 2019 (COVID-19) pandemic [1,2]. WBS can monitor the prevalence of a disease in communities or populations in advance to clinical indicators, helping in monitoring and early prevention of large disease outbreaks allowing faster decision-making by public health sector [3]. WBS consist in the detection of biomarkers present in wastewater that allow the tracking of relevant pathogenic agents that are related to the disease transmission within a population [4]. For example, monitoring viral loads of SARS-CoV-2 virus in a wastewater treatment plant from a community can traduce to the monitoring of COVID-19 spreading within the population from the community and reduce clinical testing [2,5].

In WBS the traditional sampling method is called "grab sampling" which consists of grabbing single wastewater samples to determine the amount of the desired biomarker [6]. However, biomarkers concentration such as genetic material present in wastewater can fluctuate in relation to time and the environmental conditions, generating over- or under estimation of the desired biomarker. Another method to have a more representative approach of biomarkers concentration is composite sampling which can be time consuming because of the number of samples that need to be taken at different time intervals [3,6]. Another tool that is currently being developed for WBS is the use of passive samplers which are intended to concentrate and preserve the desired biomarkers at prolonged periods of time to have a representative sampling from biomarker loads in wastewater [4,7–9]. Even there is progress in the development of passive samplers, the materials used still need to be improved, among reported materials are composed of cotton cloth, cellulose sponge, electronegative filters and activated charcoal [4]. Therefore, there is still the need to develop versatile materials that allow a better recovery rate, improved selectivity and sensitivity for the desired biomarkers.

Chitosan is a cationic biopolymer derived from the deacetylation of chitin [10–12]. The deacetylation of chitin process enhances its solubility, producing amino groups which in combination with the hydroxyl groups present in chitosan give the polymer particular characteristics that can be suitable for numerous applications [13–15]. Because of its properties such as biodegradability, non-toxicity, biocompatibility, and versatility, chitosan has been used as packing in the food industry, as wound healing implant in the biomedical industry, and in the form of hydrogels for the removal of contaminants in contaminated water [16–22].

The use of chitosan to fabricate hydrogels for contaminant removal in water is a very suitable and already adopted method because of chitosan high adsorption and binding capacity of contaminants such as metals [10,23] dyes [24,25], and other emergent contaminants of high concern such as bisphenol A (BPA) [19].

Besides the application of hydrogels for the removal of contaminants, already mentioned, biopolymer-based hydrogels have promising potential for their application as passive samplers of genetic material and their use in (WBS) [3–5]. Chitosan cationic characteristics given by the presence of amino groups can be suitable for adsorption of negatively charged genetic material like DNA or RNA molecules from pathogens present in wastewater via electrostatic interactions [11]. In fact, it is reported that chitosan inhibits RNAases activity, helping to protect RNA from degradation [26].

Also, it is important to mention, chemical modifications of amino groups by cross-linking with chitosan and other polymers can result favorable for adsorption of viral RNA/DNA molecules by improving the formation of three-dimensional networks that improve porosity and might improve superficial area for adsorption [27].

Despite all of the attributes and diversity in applications, chitosan hydrogels still need to be modified and/or improved and reach the desired mechanical and physical properties for specific applications [28]. Different formulations are based on the combination of chitosan with other polymers or components to modify physical properties and reach the desired porosity or rigidity for adsorption applications. For instance, cellulose is another biopolymer that can be used as a biosorbent. Moreover, this polymer can provide rigidity and stability to a composite chitosan hydrogel. Due to the good mechanical properties that can provide, cellulose has also been reported in tissue engineering as a scaffold to form three-dimensional networks [29,30]. Lack of side chains, and the presence of amorphous and crystalline regions in cellulose, make it a very ordered, insoluble in water and stable polymer [10]. Also, cellulose structure can be chemically modified to enhance the adsorption capacities of certain components such as heavy metals [31], anionic dyes [32] and organic compounds [33].

Other components that can be added to the hydrogel formulation to improve the porosity of hydrogels are the compounds known as "Porogens", an example of these kind of compounds is the polyethylene glycol (PEG). This polymer receives particular interest for its compatibility with chitosan and the capability to form spongy-type hydrogels [34]. Another currently applications of PEG are protecting cells during cryopreservation, protein precipitation, concentration and purification of DNA and RNA, this final property is of particular interest for the concentration and preservation of genetic material present in WBS [35,36]. Although the inclusion of other polymers can change or improve the composite properties, other factors are needed to succeed in copolymerization. It must also be considered that the characteristics of a hydrogel from a combination of different polymers depend on the fabrication conditions, in

which the different chemical groups from the polymers react creating specific interactions and chemical configurations resulting in the spatial deposition to form a 3D network [37]. Finally, the hydrogel adsorption capacity can be increased by the addition of compounds such as glutaraldehyde that acts as cross-linking between polymer chains and enhance the hydrogel mechanical properties, and chemical stability (by covalent interactions), compared to native unmodified chitosan [13,24,38]. The explored background has provided enough evidence to propose a hydrogel formulation capable of retaining gene copies from complex matrices. The present research explores hydrogel formulations based on different combinations of chitosan, cellulose, PEG and glutaraldehyde, to work as passive sampler for adsorption of genetic material from pathogens and its potential tool application for wastewater-based surveillance (WBS).

2. Materials and methods

2.1. Chemicals

Chitosan flakes of low-molecular weight (20–300 cps), with a 75 % deacetylation degree, polyethylene glycol 8000 (PEG 8000), microcrystalline cellulose and glutaraldehyde solution grade I (50 %) were purchased from Sigma-Aldrich (MO, USA). Glacial acetic acid of analytical grade was purchased from JT Baker (NJ, USA).

2.2. Hydrogel formulation

For hydrogel preparation, dry chitosan flakes were added in a solution of acetic acid (2 %) and stirred until fully dissolved to obtain a chitosan solution (1.5–2.5 % w/w). Then, every component from the formulation was solubilized sequentially, in the following order: Polyethylene glycol 8000 (PEG) (0–3%), and microcrystalline cellulose (MCC) (0–3% w/w), according to each formulation. Glutaraldehyde (0.04–0.12 % w/v) was added to the mixture at the end to carry out the cross-linking of the polymers under constant agitation. The prepared mixture was then cast on petri dishes (50 mm diameter) and incubated at 30 °C for 24 h for hydrogel gelation. After the gelation the moisture content (%) of each formulation was determined using a thermobalance (Model DSH 50–10, Roca, MEX).

2.3. Experimental design

To evaluate the effect of the different components of the formulation on the structural, mechanical, and adsorption properties, a Box-Hunter experimental matrix of 9 formulations was used (Table 1). The prepared formulations will be identified as F1 to F9 throughout the discussion in the paper.

2.4. Physicochemical characterization

Hydrogels' weight, moisture content and thickness were determined. The moisture content (%) of each formulation was determined by taking a 0.5 g sample and dried using a thermobalance at 180 °C until constant weight. Hydrogels' thickness was recorded with a Vernier micrometer (Artikelnr) taking 3 measurements from each hydrogel formulation.

2.5. Fourier transform infrared analysis (FTIR)

The FTIR test was used to assess the functional groups present in the hydrogels, chitosan along with the possible configurations carried out with the crosslinking using glutaraldehyde in combination with MCC and PEG. Fourier transform infrared spectra of different chitosan gels was carried out on an FTIR Frontier spectrometer (PerkinElmer, MA, USA). A total of 32 scans were performed in the range of 400–4000 cm^{-1}.

Table 1
List of formulations explored to evaluate hydrogel gelation and characterization.

Formulation	Chitosan	Glutaraldehyde	MCC	PEG
	% (w/w)	% (w/v)	% (w/w)	% (w/w)
F1	1.5	0.04	0	0
F2	1.5	0.12	3	3
F3	1.5	0.12	0	3
F4	1.5	0.12	3	0
F5	2.5	0.04	0	3
F6	2.5	0.04	3	0
F7	2.5	0.12	0	0
F8	2.5	0.12	3	3
F9	2	0.08	1	1

2.6. Zeta potential analysis

The surface charge of the different hydrogel formulations was assessed by the Zeta potential. Zeta potential was measured using the Zetasizer nano series (Malvern Panalytical, Almelo, NLD). All samples (1 square from each hydrogel 0.5 cm × 0.5 cm) were diluted in 10 mL of acetic acid solution (2 %) and 2 mL from the aqueous solutions were placed in the Zeta Cell for the measurements. The adjustable gap ranged from 110 to 140 μm to avoid any material swelling effect on the measurement. The zeta potential measurement was performed 3 times for each sample at a fixed pH = 3.0.

2.7. Scanning electron microscope (SEM)

Microstructural analysis from the different hydrogels was performed to see the different configurations formed from the polymers at the different concentrations from the formulations obtained by the experimental design. Different hydrogel samples were completely dried in an oven at 35 °C until constant weight. The samples surfaces were then gold-coated and cross sections of the samples were observed by scanning electron microscopy (SEM) (EVO MA 25, Zeiss, GER) at a voltage of 10 kV for the morphology analysis of the different hydrogels.

2.8. Swelling ratio (SD) of the different hydrogel formulations

The swelling ratio of all hydrogel formulations was assessed based on the method reported by Malik et al., [25]. The initial hydrogels weight was measured (*Wdry*) and then immersed in distilled water at room temperature (25 ± 0.5 °C). Then, the gels were retrieved from the water and removed the excess water with a filter paper prior to final weight measure (*Wsw*) after swelling. The weight of the swelled hydrogels (*Wsw*) was recorded at different time intervals (0, 0.5, 1, 2, 3, 6 and 24 h) to assess the swelling ratio of the different hydrogels according to the following equation:

*Swelling ratio= (Wsw – Wdry/Wdry) * 100.*

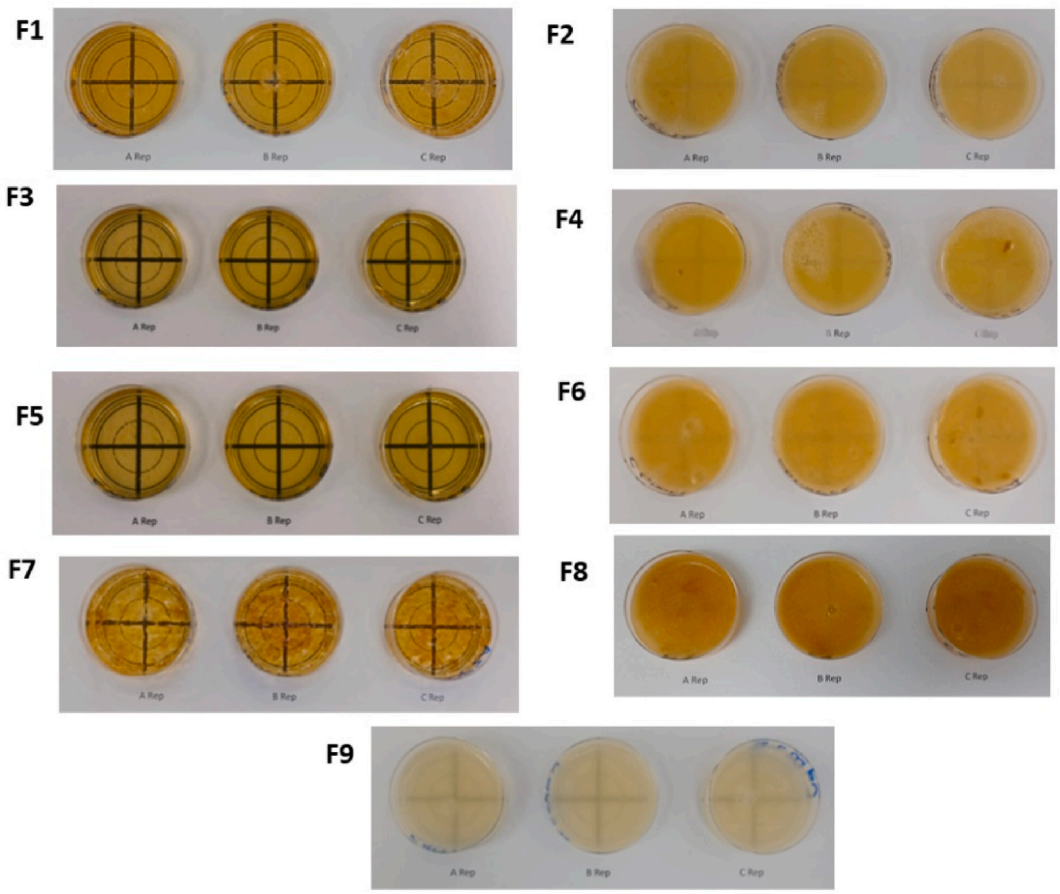

Fig. 1. Photographs of the different hydrogel formulations, each formulation has three replicates in the same row. It is visible the coloration and transparency changes thanks to the same dark cross marked in each Petri dish.

2.9. Adsorption of genetic material

The genetic material adsorption was assessed on the best hydrogel formulation in terms of the overall evaluated physicochemical properties (details in section 3, Results and Discussion). This adsorption trial was conducted based on the methodology reported by Lin et al. [27], with the modifications described below. The selected hydrogel formulation for the adsorption of genetic material was F8, composed of 2.5 % Chitosan, 3 % MCC, 3 % PEG, and 0.12 % Glutaraldehyde. A model water sample was spiked with gene M synthetic construct of Influenza A virus (inhouse designed and described ahead), carrying the sequence of Matrix M gene of the virus at a concentration of 212,040.00 Gene copies/mL (GC/mL). For the assay, hydrogels with a weight of 1 g were placed into a 50 mL conic tube with 5 mL of spiked water and incubated for 48 h at 25 °C with an orbital agitation of 1000 rpm. After the incubation samples were taken from the water, extraction of genetic material was carried out from hydrogels with MagMAX viral RNA extraction kit (Applied biosystems, MA, USA) and rt-qPCR was carried for samples from water supernatants, extracted from hydrogels, positive and negative controls using QuantStudio 5 system (Applied biosystems).

Nucleic acid extraction was performed using the MagMAX viral RNA extraction kit (Applied biosystems), according to the supplier's instructions adapted for a KingFisher™ Flex automated system (ThermoFisher, MA, USA). Eluted genetic materials were recovered and stored at −20 °C for further analysis.

Influenza A genetic material was detected and quantified through rt-qPCR using the "One step rt-PCR Super Script III platinum DNA *Taq* polymerase" (Invitrogen, thermos fisher scientific) on a QuantStudio 5 system. Reactions consisted of 0.75 μL of Influenza A mix (Matrix gene target "M) (containing M gene primers and probes), 10.75 μL of one step RNA Master Mix (Super Script III RT/Platinum *Taq* Mix (0.25 μL), reaction buffer 2× (6.25 μL), ROX reference dye (0.1 μL), nuclease free water PCR grade (4.15 μL), and 1 μL of extracted genetic material. Positive and negative controls were set alongside the assays. The rt-qPCR program consisted of an initial hold for 15min at 50 °C and 1 min at 95 °C, followed by 45 cycles of 95 °C for 15 s and 60 °C for 30s. The primers and probes to perform rt-qPCR assay were designed using Oligo Primer Analysis 7 software and NCBI Primer-BLAST platform, PCR in silico and quality checks of amplification were performed using Amplify4 software. The following sequence corresponds to 5′-AGATGAGTCTTCTAACC-GAGGTCG-3′ (forward primer), 5′-TGCAAAAACATCTTCAAGTCTCTG-3′ (reverse primer) and 5′-CCCCCTCAAAGCCGAGATCG-3′-FAM (probe).

2.10. Statistical analysis

Design of experiments and Analysis of variance comparisons was performed using software Statistica 7.0 (Statsoft). Differences were considered significant for $p < 0.05$. Experiments were carried out in triplicates and data are reported as means ± standard deviation (SD).

3. Results and discussion

The hydrogels prepared from the different formulations had an average weight of 10.10 ± 1.12 g and a thickness of 5.43 ± 0.58 mm. However, these hydrogels exhibited different physical characteristics, such as opacity differences (Fig. 1), which were increased in those where cellulose was added (F2, F4, F6, F8, and F9). These formulations presented a more opaque and dense appearance compared to the hydrogels without cellulose (F1, F3, F5, and F7), which had a translucent appearance. In addition to visual

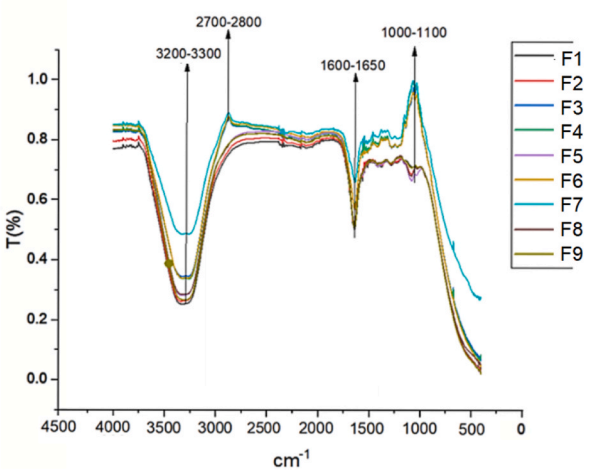

Fig. 2. FTIR spectra for each hydrogel formulation (transmittance vs wavenumber).

appearance, hydrogels with a lower chitosan concentration exhibited greater fragility upon contact. The characterization of the different hydrogel formulations is presented in the following subsections.

3.1. Fourier transform infrared analysis (FTIR)

The different formulations of hydrogels have similar FTIR spectral behavior. Fig. 2 shows the FTIR spectra in a range from 0 to 4500 cm^{-1}. Similar spectra are observed in all 9 formulations in the range of 3000–3700 cm^{-1}. This peak is associated with the stretching vibrations of O–H bonds related to the hydroxyl groups present in chitosan, microcrystalline cellulose, and PEG, overlapping the N–H stretching of chitosan [39]. In the samples with lower concentrations or absence of PEG and MCC, the signal became weaker in the spectra of the chitosan-glutaraldehyde crosslinked hydrogel, indicating the conversion of the –OH group into acetal linkage [40]. In the region of 1000–1100 cm^{-1}, a change in transmittance can be observed in F7, F6, and F4 (Fig. 5), where the amount of PEG is zero in their treatment. From this evidence, it can be inferred that the presence of PEG vibrations accounts for the amount of this material in the subsequent samples.

Furthermore, an increase in the signal is observed in the same samples in the region of 2700–2800 cm^{-1}, indicating the C–H stretching vibration from PEG compound [39]. A significant peak can be found approximately between 1600 and 1700 cm^{-1} corresponding to the formation of imine bond (C=N) forming Schiff's base structure by the reaction of amino groups of chitosan and aldehyde groups of glutaraldehyde [24]. The signals between 900 and 1100 cm^{-1} correspond to stretching vibrations of C–O–C bridges from chitosan and C–O stretching vibration from polysaccharides structures [39,41].

3.2. Scanning electron microscope (SEM)

The high-water absorption capacity can be linked to the highly porous structure from the hydrogels observed in the SEM study. The formulated hydrogels display a smooth surface on the Petri dish surface side and a rough surface on the air side of the gel. The inner structure of the hydrogels was observed by doing a lateral cut of the hydrogels evidencing the formed networks between the polymers and the incidence of wrinkles, fissures, cracks, and pores, which displayed some differences depending on the formulation (Fig. 3). The smooth surface but high porosity of F4 (504.50 ± 17.51 % swelling ratio) can be observed in Fig. 2 in which inner porous structure was observed at a magnification of 100x (spaces in the network are within 100 μm range). A tighter structure was observed in micrographs of the hydrogels from F8 (which has the highest concentration of all the components: 2.5 % Chitosan, 0.12 % Glutaraldehyde, 3 % MCC, 3 % PEG). High rugosity was observed, but pore distribution was not evident even at a magnification of 1000x. F8 is one of the formulations with a lower swelling degree (266.38 ± 17.82 %).

3.3. Zeta potential analysis

Analysis of zeta potential of chitosan hydrogels showed that all the formulations have positive surface charge, between 6.29 ± 1.53 mV and up to 35.80 ± 1.44 mV showing statistical differences between groups (as seen in Table 2). Resulting Zeta potential could be attributed mainly to the chitosan as it is reported to have positive zeta potential under acidic conditions (pH evaluated 3.0). In acidic conditions, chitosan is positively charged due to the protonation of amino groups present in its composition [42] $NH_2 + H^+$ converted to NH_3^+. It is reported that zeta potential of chitosan can vary significantly between +42 and 0 mV from pH 2 to pH 9.0 respectively, as the pH lowers, the higher the protonation of amine groups leading to more positive zeta potential and as the pH increases the zeta potential tends towards 0 or negative [43,44].

However, significant differences could be found between formulations which can be attributed to the different combinations and concentrations of MCC, PEG and glutaraldehyde. MCC and PEG might not have a significant surface charge but along with the combination of glutaraldehyde and chitosan different steric combinations can be formed, altering the morphology and the spatial

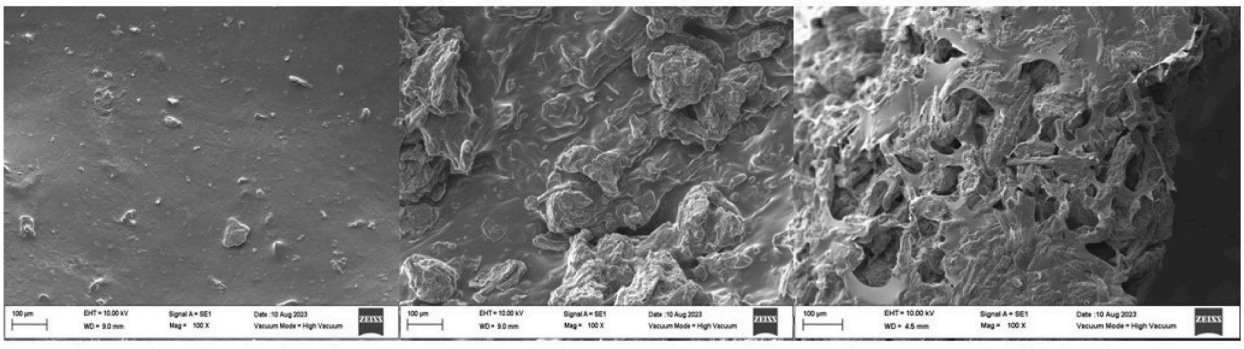

Fig. 3. SEM micrographs of the three more representative formulations at 100x magnification. Left) Surface from hydrogel (F2). Center) Inner structure of the hydrogels with the highest concentration of chitosan (F8) and Right) Inner structure of the hydrogel with the lowest concentration of chitosan (F4).

Table 2
Zeta potential of different hydrogel formulations (From lowest to highest).

Formulation	Zeta potential (mV)
F6	6.29 ± 1.53^{c}
F7	11.24 ± 2.34^{bc}
F2	18.20 ± 1.95^{b}
F3	22.95 ± 0.92^{b}
F4	27.70 ± 0.95^{ab}
F9	30.77 ± 1.53^{ab}
F1	34.23 ± 3.71^{a}
F5	35.40 ± 0.36^{a}
F8	35.80 ± 1.44^{a}

*Statistical differences between groups are represented by superscript letters. Differences were considered significant for $p < 0.05$.

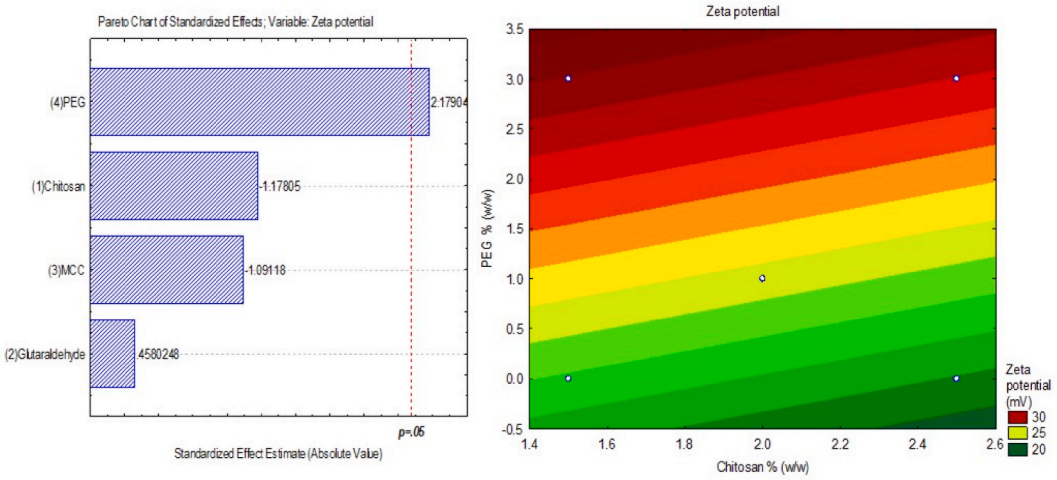

Fig. 4. Left) Pareto chart of the effects of the components on zeta potential of the hydrogels. Right) Heat map of the effect of the concentration of PEG (Y axis) and chitosan % (w/w) (x axis) on the zeta potential of the hydrogels.

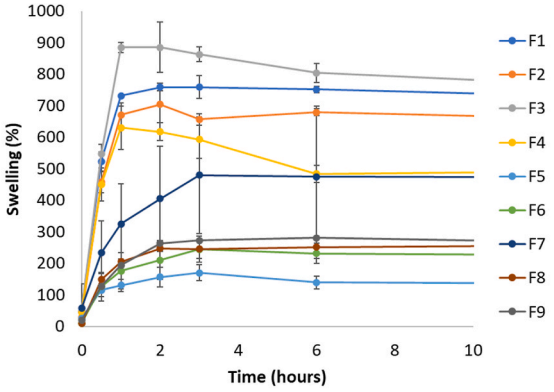

Fig. 5. Swelling dynamics of the nine experiment treatments. Note the lines extend beyond the axis length but it is not included since the swelling from 6 h. Remains approximately constant up to 24 h.

disposition of functional groups of chitosan exposition could vary depending on the generated structure given by the cross-linking process. According to statistical analysis, PEG significantly affected the zeta potential in the different hydrogel formulations (Fig. 4). Although PEG generally does not contribute significantly with its surface charges, PEG 8000 is a large, flexible molecule. When

adsorbed on the surface of colloidal particles or within a hydrogel matrix, it can form a layer that prevents the particles from approaching each other. This provides steric stability, reducing the attractive forces between particles and increasing the zeta potential.

3.4. Swelling ratio and water solubility of the hydrogels

The swelling ratio is a very important parameter because it provides information about not only the water absorption capacity of the hydrogels but also their physical behavior when placed in water. The swelling capability in relation to the polymers, as well as the degradation or solubility of the hydrogels over a prolonged period, is a crucial characteristic for their use as passive samplers [45,46]. In the results presented here, the swelling behavior showed a high-water absorption capacity for most of the hydrogels. The matrices quickly reached saturation within the first 3 h of the experiment, achieving their maximum swelling ratio, which then remained constant until 24 h (Fig. 5).

It was observed that different groups showed statistically significant differences between them at 24 h. The formulations that displayed the highest swelling ratios (F1: 693.25 ± 6.24 %, F2: 627.65 ± 11.55 %, and F3: 703.89 ± 15.00 %) belonged to those with the lowest concentration of chitosan (1.5 %) (Fig. 5) and did not contain MCC (in F1 and F3). According to the statistical analysis of the experimental design, chitosan concentration is the significant factor in the swelling phenomenon (Pareto chart Fig. 6). This group of hydrogels had a high-water absorption capacity, but their gel integrity was loose and very liquid. The statistical analysis indicates that the higher the concentration of chitosan, the lower the swelling ratio, with hydrogels from formulations with the lowest chitosan concentration swelling the most and those with the highest concentration of chitosan (2.5 %) swelling the least. Moreover, the addition of MCC and PEG displayed a negative correlation with the swelling ratio, as the inclusion of these components resulted in a lower swelling ratio. The group with formulations F6, F8, and F9 had lower swelling ratios (between 219.31 ± 59.94 % and 266.38 ± 17.82 %). However, these hydrogels maintained their integrity with only slight shape modifications, even after significant water absorption. In these formulations, the highest concentrations of chitosan (2.5 %) and MCC (3 %) were present in F8 and F6, while intermediate concentrations were found in F9 (chitosan 2 %, MCC 1 %). The effect of adding MCC in the formulations was observed in the formation of denser hydrogels. Confirmed with what it reported in literature the addition of cellulose to the hydrogel blend can improve its rigidity and stability resulting in a more compact and denser blend [10,47,48]. The effect of the concentration of chitosan and MCC in the mixtures is shown in Fig. 6, where the highest concentration of these components leads to a lower swelling ratio. With the help of the contour plot provided by the statistical analysis, a specific concentration of the polymers in the formulation can be determined based on the desired swelling ratio for specific hydrogel applications.

3.5. Adsorption of genetic material

The selected formulation for the adsorption of genetic material was F8, composed of 2.5 % Chitosan, 3 % MCC, 3 % PEG, and 0.12 % Glutaraldehyde. This formulation had the maximum swelling rate without losing physical integrity, e.g., fragmentation (Fig. S1 shows photographs of all formulations after 24 h of swelling). The characterized hydrogel formulation was evaluated to potential application as a passive sampler in wastewater-based surveillance by its capacity to capture gene copies. The results from the rt-qPCR carried out from samples retrieved from the hydrogels confirmed the capability of the hydrogels to adsorb genetic material from an artificial sample with spiked water with the gene M synthetic construct of Influenza A virus. The amplification plots from the rt-qPCR revealed the amplification of the Influenza A virus gene in the amplification cycle (Ct) 36 (Fig. 7) from the samples extracted from hydrogels which correspond to 51.96 ± 0.81 gene copies per reaction (GC/rxn), corresponding to 4157.04 ± 64.74 GC/mL (corresponding to 1.73 ± 0.03 % of genetic material adsorption) from spike water (3005.10 GC/rxn) by the hydrogel formulation sampler. Genetic material adsorption can be attributed to the several components present in the hydrogel formulation, but mainly attributed to the

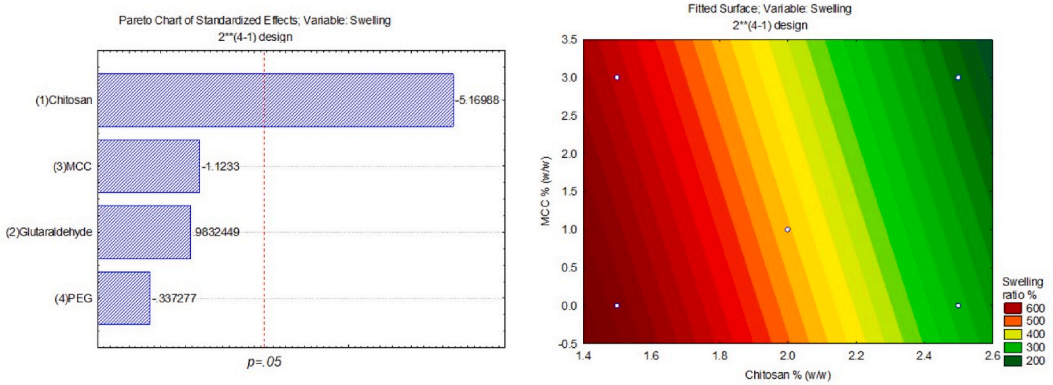

Fig. 6. Left) Pareto chart to compare the formulation four factors impacting on swelling capacity. Chitosan is statistically different from MCC, GA and PEG. Right) Heatmap plot of the impact on swelling capacity by factor in the formulation.

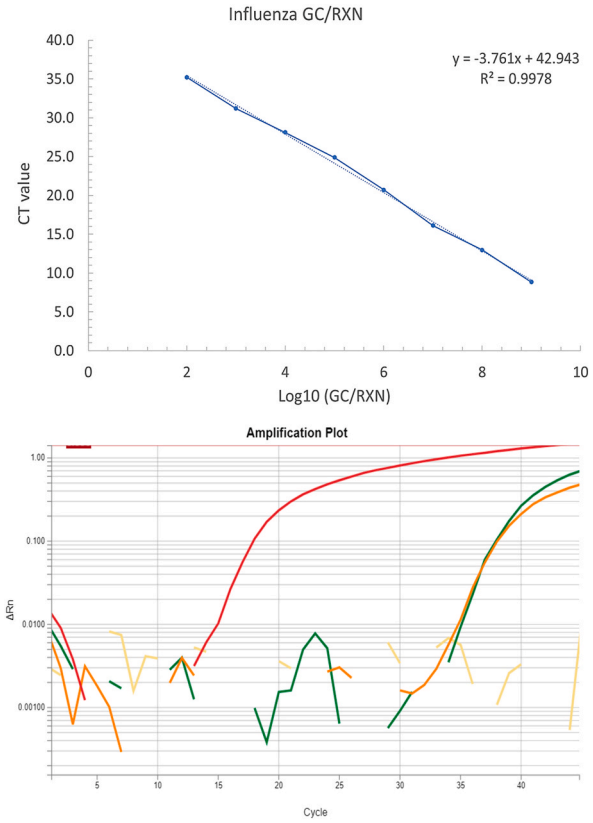

Fig. 7. Top) Calibration curve from Influenza A synthetic vector. **Bottom)** Amplification plots 366 form Influenza control (Red line), hydrogel adsorption after 24 h (Green and orange line), and 367 negative control (Yellow line). (For interpretation of the references to color in this figure legend, the reader is referred to the Web version of this article.)

electrostatic interactions as the positive charge on chitosan's amine groups can attract and bind negatively charged genetic material through electrostatic forces [11,26]. Also, chitosan and MCC hydroxyl groups [12,49] can form hydrogen bonds with the genetic material. PEG is highly hydrophilic, which can help create a hydrated environment that mimics the natural conditions in which genetic material is stable, in fact PEG is widely employed in concentration and extraction techniques in molecular biology for its properties to preserve the quality of the genetic material [35,36] (see Fig. 7).

These results represent a positive first approach for the hydrogels application as adsorbent compound in passive sampler system for genetic material adsorption, pathogen detection and their utility in surveillance protocols. The passive sampler has a low adsorption rate compared to other techniques like glass wool concentration methods, have a recovery rate of 18.8 % and 25.7 % for transmissible gastroenteritis virus (TGEV) and Hepatitis A virus (HAV) respectively [50]. However, considering that the main advantage for passive sampler implementation is to avoid the wastewater pre-treatment steps for genetic material concentration [51]. In fact, these first results help as a step towards improving the formulation and increasing the adsorption rate.

Despite the several passive samplers of genetic reports, the material applied include cotton gauze and cloths, sponges, and filter membranes, however up to date there is still not reported the use of chitosan hydrogels for its application as passive sampler for wastewater surveillance of pathogens [4,52]. Another observed advantage of chitosan over other compounds implemented in passive sampler formulation is the genetic material retention rate is higher than those reported for samplers based on zetapor, nylon, low density polyethylene (LDPE) and Polyvinylidene difluoride (PVDF) membranes, which present retention percentages of a maximum of 2.04 % for nylon membranes and a minimum of 0.24 % for LDPE membranes, using as a model the Human Norovirus Genogroup II (NoV GII) [53], similar to the retention rate (1.73 $\pm$ 0.03 %) obtained in this study with the developed hydrogel formulation used as passive sampler. However other passive samplers based in granular activated carbon (GAC) have been proved to ensure a retention rate higher than composite hydrogel, 25 % of SARS-CoV-2 genetic material in wastewater samples [8]. Higher retention rates of 24 %, 20 % and 18 % were found using membrane filter, cotton bods and gauzes-based passive samplers in wastewater samples [54]. However, in summary, the results obtained from the retention rate of the Chitosan-based hydrogel sampler can be improved, together with the retention rate background of the different passive samplers in wastewater, the retention rate of the systems confirm the suitable application of passive sampler system as feasible tools to improve the epidemiological surveillance systems robustness [53].

4. Conclusions

Different hydrogel formulations were developed and explored. The effect of different combinations and concentrations of chitosan, cellulose, and PEG was observed on the hydrogel characteristics. Overall, the different hydrogel formulations showed to display high porosity and to be highly hydrophilic displaying high swelling capacity (between 129.11 ± 9.90 % for the lowest and up to 703.89 ± 15.00 % for the highest) and positive zeta potential (between 6.29 ± 1.53 and up to 35.80 ± 1.44 mV). The effect of the concentration of chitosan, MCC and PEG was observed on the swelling ratio as higher concentration of these components led to lower swelling and more compact hydrogel structure, also observed on the network configuration on the SEM analysis. Hydrogels evaluated in the adsorption of genetic material also exhibited the capacity to adsorb genetic material in spiked water for pathogen detection by rt-qPCR assay, despite the low retention rate (4157.04 ± 64.74 GC/mL corresponding to 1.7 % of genetic material adsorption) observed of the passive sampler, the presence of chitosan in the formulation presents an opportunity to functionalize the molecule and improve the adsorption capacity. Developed hydrogels showed high potential to be used as passive samplers for pathogen detection and other contaminants present in wastewater to be part of the methodology used in WBS. The potential use of hydrogels as passive samplers suggests the further exploration of adsorption isotherms, selectivity for the desired analytes, and the potential reformulation to ensure a retention rate improvement beyond the achieved.

Funding

We are thankful to Tecnologico de Monterrey internal funding for the support of this project. This research was partially funded by the Fundación FEMSA project entitled "Unidad de respuesta rápida al monitoreo de COVID-19 por agua residual" (grant number NA), and Tecnologico de Monterrey internal funding through the project Challenge-Based Research Funding Program 2022 (Muestreador Pasivo I026 - IAMSM005 - C4-T1 - T).

CRediT authorship contribution statement

Orlando de la Rosa: Writing – review & editing, Writing – original draft, Visualization, Validation, Supervision, Software, Project administration, Methodology, Investigation, Formal analysis, Data curation, Conceptualization. **Alberto Aguayo-Acosta:** Writing – review & editing, Supervision, Software, Project administration, Methodology, Investigation, Data curation, Conceptualization. **Hiram Martín Valenzuela-Amaro:** Writing – review & editing, Software, Methodology, Investigation. **Edgar Ricardo Meléndez-Sánchez:** Writing – review & editing, Methodology, Investigation. **Juan Eduardo Sosa-Hernández:** Writing – review & editing, Supervision, Resources, Project administration, Funding acquisition, Conceptualization. **Roberto Parra-Saldívar:** Writing – review & editing, Supervision, Resources, Project administration, Funding acquisition, Conceptualization.

Declaration of competing interest

The authors declare that they have no known competing financial interests or personal relationships that could have appeared to influence the work reported in this paper.

Acknowledgments

This project acknowledges the Biotechnology Center - FEMSA and MARTEC from Tecnológico de Monterrey for the provision of the physical space for the development of the project. CONAHCYT is thankfully acknowledged for partially supporting this work under Sistema Nacional de Investigadores (SNI) program awarded to: Juan Eduardo Sosa-Hernández (CVU: 375202), Roberto Parra-Saldívar (CVU: 35753).

Appendix A. Supplementary data

Supplementary data to this article can be found online at https://doi.org/10.1016/j.heliyon.2024.e37014.

References

[1] M.D. Parkins, B.E. Lee, N. Acosta, M. Bautista, C.R.J. Hubert, S.E. Hrudey, K. Frankowski, X.-L. Pang, Wastewater-based surveillance as a tool for public health action: SARS-CoV-2 and beyond, Clinical microbiology reviews 37 (1) (2024) e0010322, https://doi.org/10.1128/cmr.00103-22.

[2] A. Amirali, K.M. Babler, M.E. Sharkey, C.C. Beaver, M.M. Boone, S. Comerford, D. Cooper, B.B. Currall, K.W. Goodman, G.S. Grills, E. Kobetz, N. Kumar, J. Laine, W.E. Lamar, C.E. Mason, B.D. Reding, M.A. Roca, K. Ryon, S.C. Schürer, B.S. Shukla, N.S. Solle, M. Stevenson, J.J. Tallon, D. Vidović, S.L. Williams, X. Yin, H. M. Solo-Gabriele, Wastewater based surveillance can be used to reduce clinical testing intensity on a university campus, Sci. Total Environ. 918 (2024), https://doi.org/10.1016/j.scitotenv.2024.170452.

[3] E.K. Hayes, M.T. Gouthro, J.J. LeBlanc, G.A. Gagnon, Simultaneous detection of SARS-CoV-2, influenza A, respiratory syncytial virus, and measles in wastewater by multiplex RT-qPCR, Sci. Total Environ. 889 (2023) 164261, https://doi.org/10.1016/j.scitotenv.2023.164261.

[4] A. Aguayo-Acosta, M.G. Jiménez-Rodríguez, F. Silva-Lance, M.A. Oyervides-Muñoz, A. Armenta-Castro, O. de la Rosa, A. Ovalle-Carcaño, E.M. Melchor-Martínez, Z. Aghalari, R. Parra-Saldívar, J.E. Sosa-Hernández, Passive sampler technology for viral detection in wastewater-based surveillance: current state and nanomaterial opportunities, Viruses 15 (2023) 1941, https://doi.org/10.3390/v15091941.

[5] A. Bivins, D. Kaya, W. Ahmed, J. Brown, C. Butler, J. Greaves, R. Leal, K. Maas, G. Rao, S. Sherchan, D. Sills, R. Sinclair, R.T. Wheeler, C. Mansfeldt, Passive sampling to scale wastewater surveillance of infectious disease: lessons learned from COVID-19, Sci. Total Environ. 835 (2022) 155347, https://doi.org/10.1016/j.scitotenv.2022.155347.

[6] M.R. Augusto, I.C.M. Claro, A.K. Siqueira, G.S. Sousa, C.R. Caldereiro, A.F.A. Duran, T.B. de Miranda, L. de M. Bomediano Camillo, A.D. Cabral, R. de Freitas Bueno, Sampling strategies for wastewater surveillance: evaluating the variability of SARS-COV-2 RNA concentration in composite and grab samples, J. Environ. Chem. Eng. 10 (2022), https://doi.org/10.1016/j.jece.2022.107478.

[7] E.K. Hayes, G.A. Gagnon, From capture to detection: a critical review of passive sampling techniques for pathogen surveillance in water and wastewater, Water Res. (2024) 122024, https://doi.org/10.1016/j.watres.2024.122024.

[8] E.K. Hayes, A.K. Stoddart, G.A. Gagnon, Adsorption of SARS-CoV-2 onto granular activated carbon (GAC) in wastewater: implications for improvements in passive sampling, Sci. Total Environ. 847 (2022) 157548, https://doi.org/10.1016/j.scitotenv.2022.157548.

[9] M. Breulmann, R. Kallies, K. Bernhard, A. Gasch, R.A. Müller, H. Harms, A. Chatzinotas, M. van Afferden, A long-term passive sampling approach for wastewater-based monitoring of SARS-CoV-2 in Leipzig, Germany, Sci. Total Environ. 887 (2023), https://doi.org/10.1016/j.scitotenv.2023.164143.

[10] S.A. Munim, M.T. Saddique, Z.A. Raza, M.I. Majeed, Fabrication of cellulose-mediated chitosan adsorbent beads and their surface chemical characterization, Polym. Bull. 77 (2020) 183–196, https://doi.org/10.1007/s00289-019-02711-4.

[11] L. Marin, B.I. Andreica, A. Anisiei, S. Cibotaru, M. Bardosova, E.M. Materon, O.N. Oliveira, Quaternized chitosan (nano)fibers: a journey from preparation to high performance applications, Int. J. Biol. Macromol. 242 (2023) 125136, https://doi.org/10.1016/j.ijbiomac.2023.125136.

[12] D.A. Marín-Silva, S. Rivero, A. Pinotti, Chitosan-based nanocomposite matrices: development and characterization, Int. J. Biol. Macromol. 123 (2019) 189–200, https://doi.org/10.1016/j.ijbiomac.2018.11.035.

[13] M.I. Wahba, Chitosan-glutaraldehyde activated calcium pectinate beads as a covalent immobilization support, Biocatal. Agric. Biotechnol. 12 (2017) 266–274, https://doi.org/10.1016/j.bcab.2017.10.016.

[14] C. Muanprasat, V. Chatsudthipong, Chitosan oligosaccharide: biological activities and potential therapeutic applications, Pharmacol. Ther. 170 (2017) 80–97, https://doi.org/10.1016/j.pharmthera.2016.10.013.

[15] C. Jeyaseelan, M. Kaur, M. Sen, Activated carbon modified chitosan beads: an effective method for removal of Congo Red dye, Mater. Today Proc. (2023), https://doi.org/10.1016/j.matpr.2023.03.802.

[16] Y. Luo, L. Cui, L. Zou, Y. Zhao, L. Chen, Y. Guan, Y. Zhang, Mechanically strong and on-demand dissoluble chitosan hydrogels for wound dressing applications, Carbohydr. Polym. 294 (2022) 119774, https://doi.org/10.1016/j.carbpol.2022.119774.

[17] H. Agusnar Suryani, B. Wirjosentono, T. Rihayat, Z. Salisah, Synthesis and characterization of poly (lactic acid)/chitosan nanocomposites based on renewable resources as biobased-material, J. Phys. Conf. Ser. 953 (2018), https://doi.org/10.1088/1742-6596/953/1/012015.

[18] K. Li, X. Yang, X. Dong, H. Cao, S. Zhuang, X. Gu, Easy regulation of chitosan-based hydrogel microstructure with citric acid as an efficient buffer, Carbohydr. Polym. 300 (2023) 120258, https://doi.org/10.1016/j.carbpol.2022.120258.

[19] M. Bilal, Z. Jing, Y. Zhao, H.M.N. Iqbal, Immobilization of fungal laccase on glutaraldehyde cross-linked chitosan beads and its bio-catalytic potential to degrade bisphenol A, Biocatal. Agric. Biotechnol. 19 (2019), https://doi.org/10.1016/j.bcab.2019.101174.

[20] Y. Lu, Z. Wang, X. kun Ouyang, C. Ji, Y. Liu, F. Huang, L.Y. Yang, Fabrication of cross-linked chitosan beads grafted by polyethylenimine for efficient adsorption of diclofenac sodium from water, Int. J. Biol. Macromol. 145 (2020) 1180–1188, https://doi.org/10.1016/j.ijbiomac.2019.10.044.

[21] J. Yu, S. Xu, G. Goksen, C. Yi, P. Shao, Chitosan films plasticized with choline-based deep eutectic solvents: UV shielding, antioxidant, and antibacterial properties, Food Hydrocolloids 135 (2023) 108196, https://doi.org/10.1016/j.foodhyd.2022.108196.

[22] E. Jakubowska, M. Gierszewska, A. Szydłowska-Czerniak, J. Nowaczyk, E. Olewnik-Kruszkowska, Development and characterization of active packaging films based on chitosan, plasticizer, and quercetin for repassed oil storage, Food Chem. 399 (2023), https://doi.org/10.1016/j.foodchem.2022.133934.

[23] R. Sesia, S. Ferraris, M. Sangermano, S. Spriano, UV-cured chitosan-based hydrogels strengthened by tannic acid for the removal of copper ions from water, Polymers 14 (2022), https://doi.org/10.3390/polym14214645.

[24] M.A. Khapre, S. Pandey, R.M. Jugade, Glutaraldehyde-cross-linked chitosan–alginate composite for organic dyes removal from aqueous solutions, Int. J. Biol. Macromol. 190 (2021) 862–875, https://doi.org/10.1016/j.ijbiomac.2021.09.026.

[25] S.A. Malik, A.A. Dar, J.A. Banday, Rheological, morphological and swelling properties of dysprosium-based composite hydrogel beads of alginate and chitosan: a promising material for the effective cationic and anionic dye removal, Colloids Surfaces A Physicochem. Eng. Asp. 663 (2023) 131046, https://doi.org/10.1016/j.colsurfa.2023.131046.

[26] M. Farrag, S. Abri, N.D. Leipzig, pH-dependent RNA isolation from cells encapsulated in chitosan-based biomaterials, Int. J. Biol. Macromol. 146 (2020) 422–430, https://doi.org/10.1016/j.ijbiomac.2019.12.263.

[27] Y.C. Lin, S.T. Lin, C.Y. Chen, S.C. Wu, Enterovirus 71 adsorption on metal ion-composite chitosan beads, Biotechnol. Prog. 28 (2012) 206–214, https://doi.org/10.1002/btpr.699.

[28] L. Tang, L. Wang, X. Yang, Y. Feng, Y. Li, W. Feng, Poly(N-isopropylacrylamide)-based smart hydrogels: design, properties and applications, Prog. Mater. Sci. 115 (2021), https://doi.org/10.1016/j.pmatsci.2020.100702.

[29] J. Xiao, Q. Wei, J. Xue, Z. Yang, Z. Deng, F. Zhao, Preparation and in vitro bioactivity study of a novel hollow mesoporous bioactive glass nanofiber scaffold, Molecules 27 (2022) 1–11, https://doi.org/10.3390/molecules27227973.

[30] J. Xiao, Q. Wei, J. Xue, Z. Liu, Z. Li, Z. Zhou, F. Chen, F. Zhao, Mesoporous bioactive glass/bacterial cellulose composite scaffolds for bone support materials, Colloids Surfaces A Physicochem. Eng. Asp. 642 (2022) 128693, https://doi.org/10.1016/j.colsurfa.2022.128693.

[31] G. Wang, T. Lu, X. Zhang, M. Feng, C. Wang, W. Yao, S. Zhou, Z. Zhu, W. Ding, M. He, Structure and properties of cellulose/HAP nanocomposite hydrogels, Int. J. Biol. Macromol. 186 (2021) 377–384, https://doi.org/10.1016/j.ijbiomac.2021.07.060.

[32] R.M. Abdelaziz, A. El-Maghraby, W.A.A. Sadik, A.G.M. El-Demerdash, E.A. Fadl, Biodegradable cellulose nanocrystals hydrogels for removal of acid red 8 dye from aqueous solutions, Sci. Rep. 12 (2022) 1–17, https://doi.org/10.1038/s41598-022-10087-1.

[33] T. Xu, Z. Wang, Y. Ding, W. Xu, W. Wu, Z. Zhu, H. Fong, Ultralight electrospun cellulose sponge with super-high capacity on absorption of organic compounds, Carbohydr. Polym. 179 (2018) 164–172, https://doi.org/10.1016/j.carbpol.2017.09.086.

[34] F. Widhi Mahatmanti, Narsito Nuryono, Adsorption of Ca(II), Mg(II), Zn(II), and Cd(II) on chitosan membrane blended with rice hull ash silica and polyethylene glycol, Indones. J. Chem. 16 (2016) 45–52, https://doi.org/10.22146/ijc.21176.

[35] P.K. Sharma, M. Halder, U. Srivastava, Y. Singh, Antibacterial PEG-chitosan hydrogels for controlled antibiotic/protein delivery, ACS Appl. Bio Mater. (2019) 5313–5322, https://doi.org/10.1021/acsabm.9b00570.

[36] S. Lee, X. Tong, F. Yang, Effects of the poly(ethylene glycol) hydrogel crosslinking mechanism on protein release, Biomater. Sci. 4 (2016) 405–411, https://doi.org/10.1039/c5bm00256g.

[37] O. Goncharuk, Y. Samchenko, L. Kernosenko, O. Korotych, T. Poltoratska, N. Pasmurtseva, O. Oranska, D. Sternik, I. Mamyshev, Thermoresponsive hydrogels physically crosslinked with magnetically modified LAPONITE® nanoparticles, Soft Matter 16 (2020) 5689–5701, https://doi.org/10.1039/d0sm00929f.

[38] M.I. Wahba, Glutaraldehyde-copper gelled chitosan beads: characterization and utilization as covalent immobilizers, Biocatal. Agric. Biotechnol. 50 (2023) 102668, https://doi.org/10.1016/j.bcab.2023.102668.

[39] R.A. Masud, M.S. Islam, P. Haque, M.N.I. Khan, M. Shahruzzaman, M. Khan, M. Takafuji, M.M. Rahman, Preparation of novel chitosan/poly (ethylene glycol)/ZnO bionanocomposite for wound healing application: effect of gentamicin loading, Materialia 12 (2020), https://doi.org/10.1016/j.mtla.2020.100785.

[40] P.G. Ingole, N.R. Thakare, K. Kim, H.C. Bajaj, K. Singh, H. Lee, Preparation, characterization and performance evaluation of separation of alcohol using crosslinked membrane materials, New J. Chem. 37 (2013) 4018–4024, https://doi.org/10.1039/c3nj00952a.

[41] J.M.F. Pavoni, N.Z. dos Santos, I.C. May, L.D. Pollo, I.C. Tessaro, Impact of acid type and glutaraldehyde crosslinking in the physicochemical and mechanical properties and biodegradability of chitosan films, Polym. Bull. 78 (2021) 981–1000, https://doi.org/10.1007/s00289-020-03140-4.
[42] K.O. Lima, C. Mauricio, B. Pinilla, M.L. Elvira, M.G. Carmen, P. Montero, C. Prentice, Characterization, bioactivity and application of chitosan-based nanoparticles in a food emulsion model, Polymers 13 (19) (2021) 3331, https://doi.org/10.3390/polym13193331.
[43] R. Athavale, N. Sapre, V. Rale, S. Tongaonkar, G. Manna, A. Kulkarni, M.M. Shirolkar, Tuning the surface charge properties of chitosan nanoparticles, Mater. Lett. 308 (2022) 131114, https://doi.org/10.1016/j.matlet.2021.131114.
[44] W. Janik, K. Ledniowska, M. Nowotarski, S. Kudła, J. Knapczyk-Korczak, U. Stachewicz, E. Nowakowska-Bogdan, E. Sabura, H. Nosal-Kovalenko, R. Turczyn, G. Dudek, Chitosan-based films with alternative eco-friendly plasticizers: preparation, physicochemical properties and stability, Carbohydr. Polym. 301 (2023), https://doi.org/10.1016/j.carbpol.2022.120277.
[45] K.I. Hoshino, T. Nakajima, T. Matsuda, T. Sakai, J.P. Gong, Network elasticity of a model hydrogel as a function of swelling ratio: from shrinking to extreme swelling states, Soft Matter 14 (2018) 9693–9701, https://doi.org/10.1039/c8sm01854e.
[46] Q. Lv, M. Wu, Y. Shen, Enhanced swelling ratio and water retention capacity for novel super-absorbent hydrogel, Colloids Surfaces A Physicochem. Eng. Asp. 583 (2019) 123972, https://doi.org/10.1016/j.colsurfa.2019.123972.
[47] S.C. Barros, A.A. da Silva, D.B. Costa, I. Cesarino, C.M. Costa, S. Lanceros-Méndez, A. Pawlicka, M.M. Silva, Thermo-sensitive chitosan–cellulose derivative hydrogels: swelling behaviour and morphologic studies, Cellulose 21 (2014) 4531–4544, https://doi.org/10.1007/s10570-014-0442-9.
[48] C.N. Elangwe, S.N. Morozkina, R.O. Olekhnovich, A. Krasichkov, V.O. Polyakova, M.V. Uspenskaya, A review on chitosan and cellulose hydrogels for wound dressings, Polymers 14 (2022), https://doi.org/10.3390/polym14235163.
[49] I.H. Sahputra, A. Alexiadis, M.J. Adams, Effects of moisture on the mechanical properties of microcrystalline cellulose and the mobility of the water molecules as studied by the hybrid molecular mechanics–molecular dynamics simulation method, J. Polym. Sci., Part B: Polym. Phys. 57 (2019) 454–464, https://doi.org/10.1002/polb.24801.
[50] A. Blanco, I. Abid, N. Al-Otaibi, F.J. Pérez-Rodríguez, C. Fuentes, S. Guix, R.M. Pintó, A. Bosch, Glass wool concentration optimization for the detection of enveloped and non-enveloped waterborne viruses, Food Environ. Virol. 11 (2019) 184–192, https://doi.org/10.1007/s12560-019-09378-0.
[51] M.V.A. Corpuz, A. Buonerba, G. Vigliotta, T. Zarra, F. Ballesteros, P. Campiglia, V. Belgiorno, G. Korshin, V. Naddeo, Viruses in wastewater: occurrence, abundance and detection methods, Sci. Total Environ. 745 (2020) 140910, https://doi.org/10.1016/j.scitotenv.2020.140910.
[52] E.K. Hayes, C.L. Sweeney, M. Fuller, G.B. Erjavec, A.K. Stoddart, G.A. Gagnon, Operational constraints of detecting SARS-CoV-2 on passive samplers using electronegative filters: a kinetic and equilibrium analysis, ACS ES T Water 2 (2022) 1910–1920, https://doi.org/10.1021/acsestwater.1c00441.
[53] F. Vincent-Hubert, B. Morga, T. Renault, F.S. Le Guyader, Adsorption of norovirus and ostreid herpesvirus type 1 to polymer membranes for the development of passive samplers, J. Appl. Microbiol. 122 (2017) 1039–1047, https://doi.org/10.1111/jam.13394.
[54] J. Habtewold, D. McCarthy, E. McBean, I. Law, L. Goodridge, M. Habash, H.M. Murphy, Passive sampling, a practical method for wastewater-based surveillance of SARS-CoV-2, Environ. Res. 204 (2022), https://doi.org/10.1016/j.envres.2021.112058.